# Lipids as therapeutic targets for barrier repair in skin diseases

Boiten, W.A.

# Chapter 3

# Compromising human skin *in vivo* and *ex vivo* to study skin barrier repair

**Authors and affiliations:**

W.A. Boiten[a]*, T. Berkers[a]*, S. Absalah[a], J. van Smeden[a,b], A.P.M. Lavrijsen[c], J.A. Bouwstra[a]

[a]Department of Drug Delivery Technology, Cluster BioTherapeutics, Leiden Academic Centre for Drug Research, Leiden University, Leiden, the Netherlands

[b]Current address: Centre for Human Drug Research, Leiden, The Netherlands.

[c]Department of Dermatology, Leiden University Medical Centre, Leiden, the Netherlands

* Both authors contributed equally to this work

**Published as and adapted from:**
Biochim Biophys Acta Mol Cell Biol Lipids. 2019 Aug;1864(8):1103-1108

**Background**
Chromatograms of selected ceramides in samples from *ex vivo* and *in vivo* SC (left and rigth, respectively)

# 3

# *In vivo* and *ex vivo* skin barrier repair


## Abstract

To study skin with a compromised barrier, regenerated stratum corneum (SC) of cultured *ex vivo* skin can be used as a model. Yet, it needs to be established how close regenerated SC models mimics the lipid composition and lipid ordering of regenerated humans SC *in vivo*. Using a comprehensive ceramide analysis method we examined whether human *ex vivo* regenerated SC showed similar ceramide alterations as human *in vivo* regenerated SC. Both *in vivo* and *ex vivo* regenerated SC had increased percentages of sphingosine ceramide subclasses and decreased percentages of phytosphingosine ceramide subclasses, a reduced mean ceramide chain length, and a higher percentage of unsaturated ceramides. Predictive data modeling using the lipid parameter showed that changes in lipid organization were party explained by changes in ceramide composition. Overall, regenerated SC *ex vivo* showed more pronounced but similar changes compared to the *in vivo* response. One of the purposes of these skin models is to use them to mimic the compromised skin of inflammatory skin diseases. The altered lipid properties in regenerated SC were comparable to those observed in several inflammatory skin diseases, showing they can be applied as models to study barrier properties in inflammatory skin diseases.


## Highlights;

- Ceramide compositions of *in vivo* and *ex vivo* regenerated stratum corneum were affected similarly
- Modeling could partly predict changes in lipid ordering
- Changes in ceramide composition in both models reflects that of inflamed skin


**keywords:**
Regenerated
Stratum corneum;
Skin;
Human *in vivo*;
Cultured *ex vivo;*
Mass spectrometry;

## 3.1 Introduction

The main skin barrier function is located in the uppermost epidermal layer, the stratum corneum (SC). This layer consisting of terminally differentiated corneocytes embedded in a lipid matrix [1]. A proper lipid organization and lipid composition in this matrix are important for a well-functioning skin barrier[2-4]. The SC barrier lipids (e.g. ceramides, fatty acids, and cholesterol) are mainly assembled in a dense orthorhombic lateral packing while a smaller lipid fraction adopts a less dense hexagonal packing[5,6]. The SC ceramide fraction consists of a specific set of ceramide subclasses defined by their sphingoid base and acyl chain. Both chains can vary in carbon chain length and polar head group, resulting in a wide array of differently structured ceramide species (**Supplemental S3.1**).

Tape-stripping healthy human *in vivo* skin is a method to compromise the SC barrier and can be used as: a model to study several aspects of inflammatory skin diseases[7], to examine the penetration of compounds through the skin[8,9], to increase the bioavailability of topical products at the deeper epidermal layers[10], and to examine the biological processes of skin barrier repair[11-13]. One of these processes is restoring the lipid composition and lipid ordering in the SC. However, little is known about the effect of barrier disruption and SC regeneration on the lipid properties of the SC and whether the regenerated SC lipid properties mimic healthy or diseased skin.

An alternative model to study skin barrier repair is using cyanoacrylate stripped *ex vivo* skin which regenerates SC over time in an incubator, this model is named the skin barrier repair (SkinBaR) model[14]. Several aspects of this model have been studied and are known to mimic, to some extent, the lipid properties of inflammatory skin diseases[14,15]. However, it is unknown to what extent the ceramide composition of the SkinBaR model reflects that of tape-stripped and regenerated human skin *in vivo*. In the present study we examine how the SkinBaR model translates to skin barrier repair studies in clinical settings. Therefore, we determined the ceramides composition and lipid ordering in regenerated SC of the *ex vivo* SkinBaR model and in regenerated SC of *in vivo* tape-stripped skin. Using statistical modeling we were able to determine and compare the effects sizes of SC regeneration in the SkinBar model to human *in vivo*, examining different parameters of the ceramide composition. Both *in vivo* and *ex vivo* regeneration altered the ceramide composition and mimicked important aspects of the ceramide composition encountered in atopic dermatitis (AD).

## 3.2 Materials & Methods

### *3.2.1 Examining the compromised in vivo skin barrier*

A clinical study was setups in which 15 healthy Caucasian volunteers between 18-29 years old participated. The study was approved by the medical ethical committee of Leiden University Medical Center and performed according to the Declaration of Helsinki. All volunteers signed written informed consent. To exclude interference with topical products, the volunteers were asked not to use soaps or cosmetics on their ventral forearms during the whole study period and one week prior to the study. At the start of the study the SC was disrupted by tape-stripping an area of 3.5 x 2.5 cm on the ventral forearm using D-Squame tape (CuDerm, Dallas, TX). Tape-striping continued until trans-epidermal water loss (TEWL) > 60 g/m$^2$/h and the skin had a shiny appearance[16]. TEWL was measured using an AquaFlux AF200 (Biox, London, UK). After 16 days of recovery, 21 tape-strips were harvested at the regenerated site and a control site at the same arm using polyphenylene sulfide tape (Nichiban, Tokyo, Japan). The first tape-strip was discarded. An infrared spectrum was recorded after every other tape-strip in order to examine the lipid ordering (see below). The *in vivo* samples obtained from control skin SC and SC regenerated after tape-stripping are abbreviated as Ctrl$^{in\ vivo}$ and Reg$^{in\ vivo}$

### *3.2.2 Ex vivo human skin (SkinBaR) model*

*Ex vivo* human skin was obtained from a local hospital, used within 12 hours after surgery, and handled according to the Declaration of Helsinki principles. Skin from 3 different donors was used in these experiments. For the SkinBar model, skin was cleaned, processed, cyanoacrylate stripped, and cultured as described before[14]. SkinBar and *ex vivo* SC was isolated and SC sheets were stored over silica gel under argon atmosphere until use for ceramide extraction or infrared spectroscopy (see below). SC obtained directly from *ex vivo* control skin, cultured SkinBar skin, and regenerated cyanoacrylate stripped SkinBar skin is hereafter called Ctrl$^{ev\ vivo}$, Cul$^{ex\ vivo}$, and Reg$^{ex\ vivo}$, respectively. Different numbers of samples for each donor were prepared for each of these conditions.

### *3.2.3 Ceramide analysis by LC/MS*

Lipid extraction, liquid chromatography combined with mass spectrometry (LC/MS) measurements, and quantification of tape-strips and SC sheets was performed as described elsewhere[17]. The obtained tape-strips were punched to Ø 16 mm and extracted using a modified 4 step Bligh and Dyer at 40°C. Extracts of tapes 5-8 were combined in one sample. After extraction and evaporation of the extraction solvents,

samples were dissolved in heptane:chloroform:methanol (95:2.5:2.5)(v:v:v). Ceramides were analyzed using an Acquity UPLC H-class (Waters, Milford, MA) connected to an XEVO TQ-S mass spectrometer (Waters, Milford, MA). Processing and post-processing were performed as described before[17]. The total molar amount of all ceramides was determined quantitatively and used to calculate the molar percentage of each individual ceramide. The analyzed ceramide subclasses are depicted in **Supplemental S3.1**. Ceramides standards used for calibration are listed in **Supplemental S3.2**.

### *3.2.4 Lateral organization and conformational ordering of the SC lipids*

Fourier-transform infrared spectroscopy (FTIR) was used to examine the SC lateral lipid organization and the conformational ordering of the SC lipids of *in vivo* and *ex vivo* skin samples[18]. All FTIR spectra were recorded using a Varian 670-IR spectrometer (Agilent Technologies, Santa Clara, CA). For more details see the **Supplemental S3.12**.

### *3.2.5 Statistical analyses*

SPSS (v23, IBM, New York, NY) was used for group-wise comparisons using linear mixed models (LMMs). LMMs were used because of the advantages of I) analysis of multiple variables and their interactions in one model, II) data pairing (e.g. multiple conditions within one subject) can be examined, III) the ability to handle missing data, and IV) the use of nested variables. LMMs were used to examine differences between the $Ctrl^{in\ vivo}$ and $Ctrl^{ex\ vivo}$ and the effect of SC regeneration. The effect of culturing was examined comparing $Ctrl^{ex\ vivo}$ and $Cul^{ex\ vivo}$. **Figure 3.1** depicts the different sample groups. For more details see **Supplemental S3.12**.

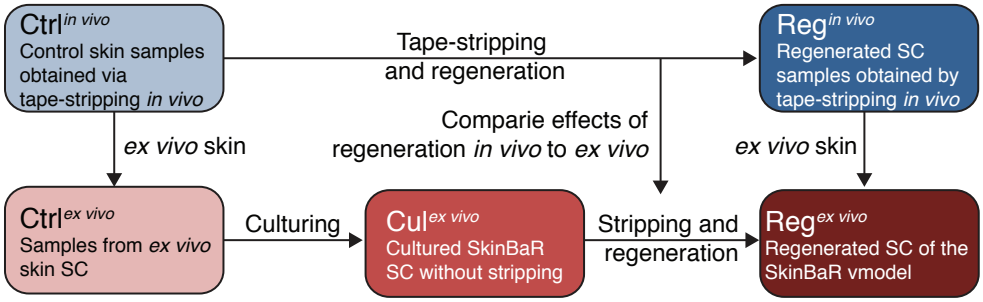


***Figure 3.1: Samples and model used to compare regeneration in vivo to ex vivo***

*Five different sample types are indicated: $Ctrl^{in\ vivo}$ and $Ctrl^{ex\ vivo}$ are the SC samples either obtained for healthy human volunteers or ex vivo SC, respectively. $Reg^{in\ vivo}$ and $Reg^{ex\ vivo}$ are samples form SC regenerated after tape or cyanoacrylate stripping, respectively. $Cul^{ex\ vivo}$ is SC from non-stripped SkinBar cultures. The effect of regeneration in vivo was determined by the difference between $Ctrl^{in\ vivo}$ and $Reg^{in\ vivo}$. The effect of regenerating ex vivo SC was determined by the difference between $Cul^{ex\ vivo}$ and $Reg^{ex\ vivo}$. The effects of regeneration in vivo and ex vivo were compared using linear mixed modelling.*

## 3.3 Results

To examine if SC regeneration induced changes in ceramide profile and whether SC regenerated *ex vivo* was similarly affected by regeneration as *in vivo* skin SC, the SC ceramide of the tape-strips obtained in the *in vivo* study and the *ex vivo* isolated SC were quantified. The following compositional parameters were examined: ceramide subclasses molar percentage (**Supplemental S3.1** explains abbreviations used for ceramide subclasses according to Motta et al.[19]), mean carbon chain length (MCL, total number of carbon atoms of both sphingoid base and acyl chain), the percentage of ceramides with a total chain length of 34 carbon atoms (C34 ceramides), and ceramides with a monounsaturated acyl chain (MuCers). We focus on these parameters as they correlated with skin barrier function in previous studies[3,12,20,21].

### *3.3.1 SC regeneration changed the ceramide subclass profile*

**Figure 3.2A and B** show the ceramide profile of all sample groups. Similar trends due to regeneration in both *in vivo* and *ex vivo* SC were observed ($Reg^{in\ vivo}$ vs. $Ctrl^{in\ vivo}$ and $Reg^{ex\ vivo}$ vs. $Cul^{ex\ vivo}$). Both *in vivo* and *ex vivo* regenerated SC showed increased S ceramide subclass and decreased P ceramide subclass percentages. Using LMMs, differences between *in vivo* and *ex vivo* SC regeneration were compared and statically tested. **Supplemental S3.3** depicts effects size of regeneration *in vivo* for each subclass. This showed that most subclasses levels were affected similar by regeneration, except for subclasses AH and EOH which had only decreased *ex vivo* and NdS and EOS which were only affected *in vivo*. Regenerations *ex vivo* gave similar but larger changes in NS, EOdS, EOP and OS subclasses levels. Culturing ($Cul^{ex\ vivo}$ vs. $Ctrl^{ex\ vivo}$) affected the ceramide subclass in a similar way as regeneration did. Overall the control conditions $Ctrl^{in\ vivo}$ and $Ctrl^{ex\ vivo}$ had comparable subclass distributions, except for subclass NP, AH, EOdS, EOP, and OH. Changes in subclass AP and NH are common donor variations and EOdS, EOP and OH subclasses occur at sub one molar percentage levels, concluding, that control conditions were similar enough for a reliable comparison of regeneration effect sizes.

The percentage of linoleate esterified omega-hydroxyl acyl ceramides (EO ceramides) changed due to regeneration and was increased *in vivo* and decreased *ex vivo* (**Figure 3.2C** and **Supplemental S3.4**). However, the percentage of ceramides with an omega-hydroxyl chain (O ceramides) increased by *ex vivo* regeneration. The total percentages of ceramides with an omega-hydroxyl chain, either acylated or not, was not affected by regeneration *ex vivo*. EO ceramides are an important factor contributing to the MCL.

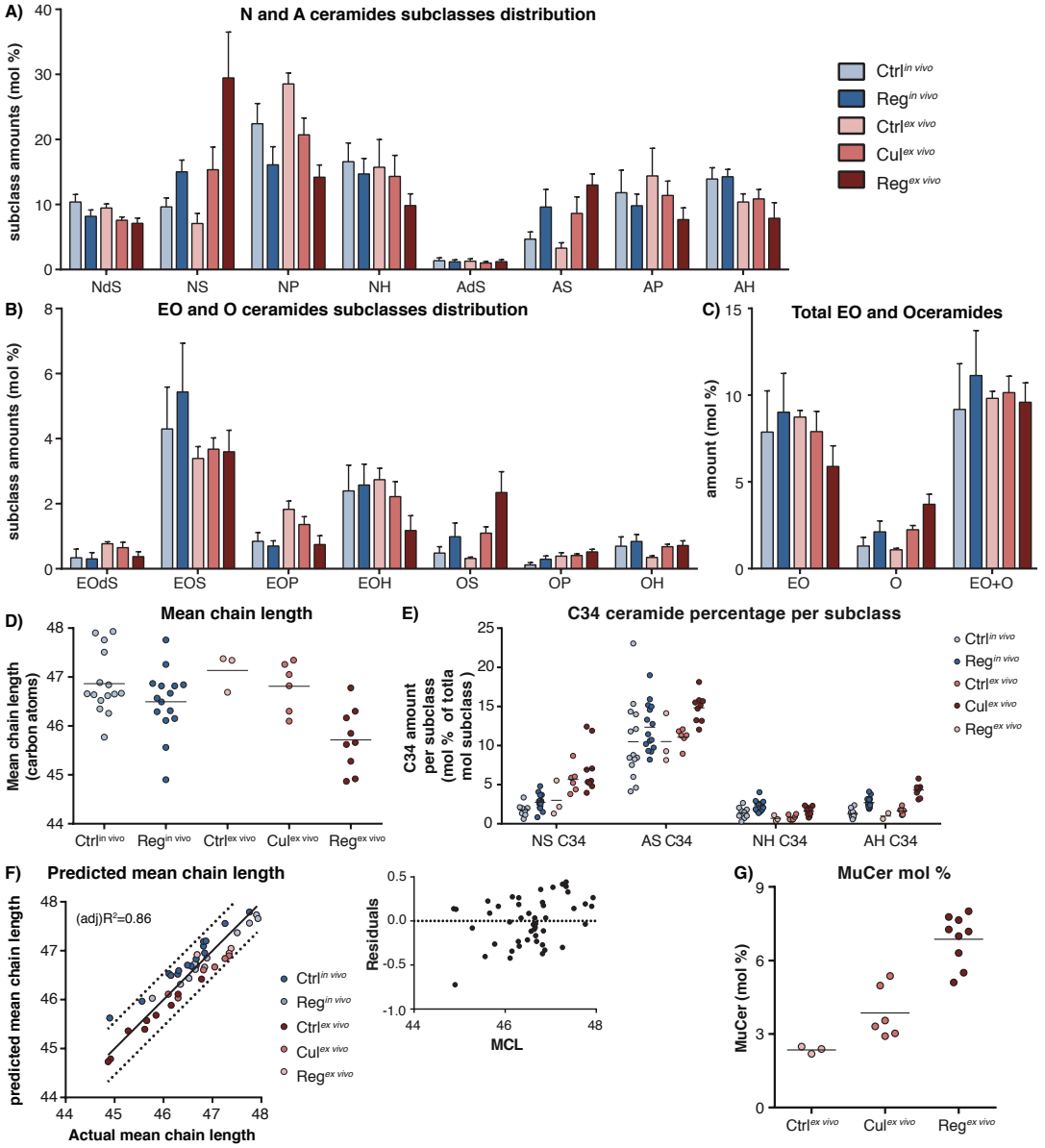


***Figure 3.2: Changes in ceramide composition.***

***A,B:*** *Subclass amount as molar percentage of the total molar amount of ceramides in a sample.* ***C:*** *Molar percentage of EO ceramides, O ceramides, and combined compared to total ceramide amount in a sample. Bars are mean +SD (n=15 for in vivo samples, n=3, 6, and 9 for Ctrlex vivo, Cul ex vivo,, and Reg ex vivo, respectively).* ***D:*** *Mean carbon chain length of all samples.* ***E:*** *The molar percentage of C34 ceramides compared to the total molar amount of its subclass. F: The mean chain length plotted against the model predicted mean chain length. Dotted lines are 95% predictive interval around a linear regression (intercept 0:0). To the right the residuals of the model are shown.* ***G:*** *Molar percentage of ceramides with monounsaturated acyl chain compared to the total ceramide amount. Lines are the mean of the sample group.*

### *3.3.2 Mean chain length and ceramides with a C34 chain length*

Changes in MCL were expected because the EO ceramides percentage increased. The MCL of all ceramides was calculated (**Figure 3.2D** and **Supplemental S3.4**). Regeneration of the SC significantly reductions the MCL. Although, both *in vivo* and *ex vivo* regeneration reduced the MCL, it was significantly more deceased in *ex vivo* SC. Culturing did not significant alter the MCL compared to $Ctrl^{ex\ vivo}$.

A parameter which has been linked to barrier dysfunction as well is the percentage of C34 ceramides. Regeneration and culturing both increased the total C34 ceramides percentage. Effects of regeneration were significantly larger in *ex vivo* than *in vivo SC*, while $Ctrl^{in\ vivo}$ and $Ctrl^{ex\ vivo}$ had similar percentages of C34 ceramides (**Supplemental S3.5 and S3.6**). To determine if the increase in C34 ceramide fraction was independent of changes in subclass (the increased S subclasses contain the most C34 ceramides), the C34 percentages within each subclass was determined. **Figure 3.2E** depicts the molar C34 ceramide percentage within subclasses NS, AS, NH and AH. Comparable increases of C34 ceramides were observed for each subclass in both $Reg^{in\ vivo}$ and $Reg^{ex\ vivo}$ compared to $Ctrl^{in\ vivo}$ and $Cul^{ex\ vivo}$, respectively (**Supplemental S3.7**). The F-test of the fixed effect for regeneration specifies that regeneration has a significant effect on C34 ceramide percentage independent of sample type or subclass. For ceramide subclasses NP, NdS, AP, and AdS a similar increase was observed but only in *ex vivo* SC (**Supplemental S3.5B**). Due to the limited amount of SC acquired by tape-stripping these ceramide subclasses fall below the quantification limit *in vivo*. Culturing did increase the C34 percentage within subclasses and the percentage did not significantly differ for $Ctrl^{in\ vivo}$ and $Ctrl^{ex\ vivo}$. It can thus be concluded that the C34 ceramide percentage is affected by regeneration independently of subclass and this is comparable between *in vivo* and *ex vivo* SC.

The C34 ceramide percentage together with EO ceramide percentage showed strong correlations to the MCL in previous studies[3]. A generalized linear model was created to predict the MCL using these parameters as covariates. **Figure 3.2F** displays the model predicted MCL against the calculated MCL and the residuals (model output can be found in **Supplemental S3.8**). The model had an adjusted $R^2$ of 0.87, indicating that 87% of the variation in MCL could be explained by the change in EO ceramides and C34 ceramides percentage and this was independent of sample type.

### *3.3.3 Ceramides with an unsaturated acyl chain*

It was previously observed that MuCers were increased in the SkinBar model[17] and MuCers might be affected by regeneration too. Although MuCers were detected in *in vivo* tape-stripped samples, these could not be accurately determined for all samples. The MuCer percentages of in the *ex vivo* groups are depicted in **Figure 3.2G**. It was

observed that MuCers significantly increased in Cul$^{ex\ vivo}$ samples and even further due to regeneration (**Supplemental S3.9**).

### *3.3.4 SC regeneration does not affect lipid ordering*

The lipid ordering was analyzed using FTIR. For the *ex vivo* samples $CH_2$ stretching vibrations in the FTIR spectra could be obtained over a temperature range from 0 to 90°C. In order to compare these results to those from *in vivo* studies, the lipid ordering at skin temperature (32°C) was examined using the center of gravity of the $CH_2$ symmetric stretching vibration peak in the FTIR spectra. A peak position below 2850 $cm^{-1}$ indicates a conformational ordering of the lipids and higher values indicated disordering. **Figure 3.3A** depicts the stretching peak position for all the samples and **supplemental S3.10** depicts the output of a LMM comparing the sample groups. The $CH_2$ peak position was not affected by regeneration. For the Ctrl$^{ex\ vivo}$ samples the peak position was located at wavenumbers of 2849.2 $cm^{-1}$, respectively, which was significantly higher than in the spectra of the *in vivo* samples.

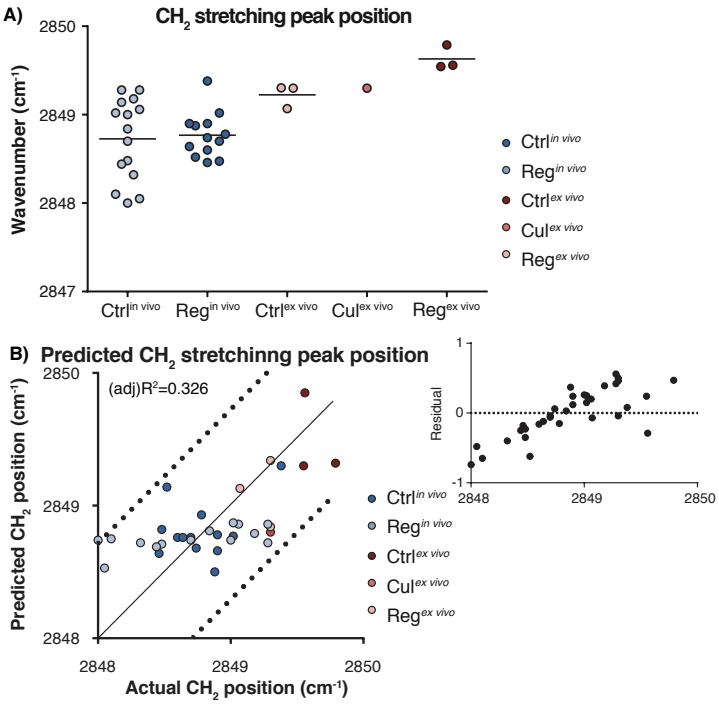


***Figure 3.3: CH2 symmetric stretching vibrations in spectra of in vivo skin and SkinBaR models and correlation of predicted values for the $CH_2$ stretching peak with observed values.***

***A:*** *The $CH_2$ stretching peak positions in the FTIR spectra. Lines indicate the mean of the sample group.* ***B:*** *The measured $CH_2$ stretching peak position compared to the model predicted $CH_2$ stretching peak position. Sample groups are indicated by color and the dotted lines are 95% predictive interval around a linear regression (intercept 0:0). To the right the residuals of the model are shown. The adjusted $R^2$ is given.*

### *3.3.5 Using ceramide composition to predict the lipid ordering*

Due to the relation between the lipid composition and conformational ordering, the difference between the conformational ordering of the lipids in the SC of the *in vivo* and *ex vivo* samples might be explained by changes in lipid composition. To obtain insight in the contribution of ceramide compositional parameters, a predictive general linear model for the lipid ordering was made (i.e. $CH_2$ stretching peak position). The following parameters were used I) C34 ceramides percentage, II) EO ceramide percentage, and III) the molar ratio between the sphingoid bases as: dS+P+H/S (excluding EO ceramides). This ratio was shown to correlate with barrier function in a previous study[12]. For more details about the subclass ratio, see **Supplemental S3.12**. **Figure 3.3B** depicts the measured $CH_2$-peak position compared to the predicted position, the inlay show the residual of the data. An adjusted $R^2$ of 0.36 that some variation in lipid ordering could already be explained using these ceramide parameters and two variables correlated significantly to the changes in lipid ordering (**Supplemental S3.11**).

## 3.4 Discussion

Important for the validity of a skin models is the translatability to physiological conditions. Here, we examined the translation to physiological conditions of the preciously developed SkinBar model[14] to the human *in vivo* situation with a focus on the SC lipids and SC regeneration.

### *3.4.1 ex vivo regenerations SC causes similar lipid alterations as regeneration in vivo*

The ceramide composition and lipid properties were altered due to regeneration and these alterations were comparable between *in vivo* and *ex vivo* conditions. Some changes observed were more pronounced in *ex vivo* SC. The processes behind some of the lipid alterations are discussed below.

I) Both *in vivo* and *ex vivo* regenerated SC showed a decreased molar percentage of phytosphingosine ceramide subclasses and increased percentage of sphingosine ceramide subclasses compared to control SC samples. This indicates an imbalance in activity of the enzymes acid sphingomyelinase and glucocerebrosidase, both involved in post-synthetic modification[22] or in alterations in ceramide synthesis. Although the expression of the post synthetic modifying enzymes was not affected in the SkinBaR model[14], their activity could have been altered[23];

II) In agreement previous observations[17], the MuCers percentage was increased

in Reg$^{ex\ vivo}$ SC. This increase coincides with an increased expression of Stearoyl-CoA desaturase in the SkinBaR model[14]. This is a lipid processing enzyme responsible for hydrocarbon chain unsaturation;

III) The only substantial difference between the *in vivo* model and *ex vivo* model was the change in EO ceramides percentages, which was increased in the Reg$^{in\ vivo}$ samples and decreased in the Reg$^{ex\ vivo}$ samples. The total percentages of ceramides with an omega hydroxyl chain (EO and O ceramides subclass) were comparable to *in vivo* SC, indicating that lineolate esterification could have been affected in *ex vivo* regenerated SC.

IV) In both *in vivo* and *ex vivo* conditions regeneration did not significantly affected the lipid ordering. In the SkinBar samples this might be due to lesser stripping depth in the present study compared to previous studies. Previously, lipids in the regenerated SC of the SkinBaR model were less ordered when almost all SC was removed[15]. The difference in $CH_2$ stretching peak position between Ctrl$^{in-vivo}$ and Ctrl$^{ex\ vivo}$ was significant and possibly due to a difference in spectrum collection methods. Nonetheless, the ceramide composition could be used to predict part of the variation in the lipid ordering. The residual error does indicate that many other factors influence the peak position



### *3.4.2 Epidermal proliferation in vivo and ex vivo*

Previously, it has been shown that in clinical settings the proliferation rate immediately after barrier disruption is higher than after a recovery period of several days and remained elevated for at least 10 days[7]. This may be caused by an inflammatory response in healthy *in vivo* skin during skin barrier repair that slows down the repair process[24]. As culturing *ex vivo* already induced similar changes in ceramide composition as regeneration, it can be hypothesized that culture conditions stimulate regeneration. Although, Cul$^{ex\ vivo}$ samples have a decreased proliferation index they do not shed SC and do not require addition SC generation. Eight days after cyanoacrylate stripping proliferation is at the same level as Ctrl$^{ex\ vivo}$ skin indicating that barrier repair is still ongoing [14], as it expected to decrease due to culturing. Since barrier function recovery of stripped healthy human skin takes at least 14 days[25] (although longer recovery times have been observed in chapter 4 of this thesis), this period and the period of 8 days in the SkinBaR model are sufficient long to study the effect of formulations on skin barrier repair.

### *3.4.3 Changes ceramide composition of regenerated SC are similar to those in inflammatory skin diseases*

It was shown that tape-stripping healthy skin induced parakeratosis[7], and induced an inflammatory response by secretion of various cytokines[26,27]. Some of these cytokines also play a role in AD and/or psoriasis[28,29] and have been shown to induce changes in the lipid biosynthesis in the viable epidermis, such as a reduction in lipid chain length, also observed in the present study[30,31]. When comparing the lipid properties of regenerated SC to that in SC of inflammatory diseased skin, many similarities were observed. These were I) similar changes in ceramide subclasses composition[20], II) a decreased MCL [32], III) an increase in percentages of C34 ceramides[20,32], and IV) an increased percentage of unsaturated lipids[33]. Most of these changes correlated with an impaired skin barrier function[3,12,20]. Although the degrees of changes vary, many of these alterations in ceramide composition have also been observed in other inflammatory skin diseases like psoriasis, and Netherton syndrome[31,34]. Additionally, a less dense lipid packing observed in Reg$^{ex\ vivo}$ SC[15] also corresponds to findings in SC of these inflammatory skin diseases: a higher fraction of lipids adopting a less dense hexagonal lateral packing has been reported[35]. The present study focused on the composition and organization of the free extractable lipids, yet we acknowledge that the bound ceramides are an important part of the stratum corneum. Analysis of the bound ceramides might be the subject of future studies.

## 3.5 Conclusion

This study shows that the changes in lipid properties in both the Reg$^{ex\ vivo}$ and Reg$^{in\ vivo}$ models are comparable and mimic the lipid properties in inflammatory skin diseases. This concerns changes in ceramide subclass profiles, C34 ceramides, MCL, and conformational ordering. Therefore, the SkinBaR model can be used to predict the *in vivo* response with regards to the lipid composition after application of topical barrier repair treatments aiming to restore the normal ceramide composition. By doing so, the need for clinical studies is reduced.

*Acknowledgement*

The authors would like acknowledge Gert Gooris for his help with programming the FTIR method. The authors express their gratitude to Evonik for supplying the synthetic CERs. This research was financially supported by Dutch Technology Foundation TTW (grant no. 12400).

**References:**


1 Michaels, A. S. C., S.K.; Shaw J.E. Drug permeation through human skin – theory and in vitro experimental measurement. *American Institute of Chemical Engineers Journal* **21**, 12 (1975).

2 Mojumdar, E. H., Kariman, Z., van Kerckhove, L., Gooris, G. S. & Bouwstra, J. A. The role of ceramide chain length distribution on the barrier properties of the skin lipid membranes. *Biochim Biophys Acta* **1838**, 2473-2483 (2014).

3 Janssens, M. *et al.* Increase in short-chain ceramides correlates with an altered lipid organization and decreased barrier function in atopic eczema patients. *J. Lipid Res* **53**, 2755-2766 (2012).

4 Jennemann, R. *et al.* Loss of ceramide synthase 3 causes lethal skin barrier disruption. *Hum Mol Genet* **21**, 586-608 (2012).

5 Pilgram, G. S., Engelsma-van Pelt, A. M., Bouwstra, J. A. & Koerten, H. K. Electron diffraction provides new information on human stratum corneum lipid organization studied in relation to depth and temperature. *J. Invest Dermatol* **113**, 403-409 (1999).

6 Damien, F. & Boncheva, M. The extent of orthorhombic lipid phases in the stratum corneum determines the barrier efficiency of human skin in vivo. *J. Invest Dermatol* **130**, 611-614 (2010).

7 Gerritsen, M. J., van Erp, P. E., van Vlijmen-Willems, I. M., Lenders, L. T. & van de Kerkhof, P. C. Repeated tape stripping of normal skin: a histological assessment and comparison with events seen in psoriasis. *Arch. Dermatol. Res* **286**, 455-461 (1994).

8 Wu, X., Biatry, B., Cazeneuve, C. & Guy, R. H. Drug delivery to the skin from sub-micron polymeric particle formulations: influence of particle size and polymer hydrophobicity. *Pharm Res* **26**, 1995-2001 (2009).

9 Gao, Y., Wang, X., Chen, S., Li, S. & Liu, X. Acute skin barrier disruption with repeated tape stripping: an in vivo model for damage skin barrier. *Skin Res Technol* **19**, 162-168 (2013).

10 Dickel, H. *et al.* Standardized tape stripping: a practical and reproducible protocol to uniformly reduce the stratum corneum. *Skin Pharmacol Physiol* **23**, 259-265 (2010).

11 Ghadially, R., Brown, B. E., Sequeira-Martin, S. M., Feingold, K. R. & Elias, P. M. The aged epidermal permeability barrier. Structural, functional, and lipid biochemical abnormalities in humans and a senescent murine model. *J Clin Invest* **95**, 2281-2290 (1995).

12 Boiten, W. A. *et al.* Applying a vernix caseosa based formulation accelerates skin barrier repair by modulating lipid biosynthesis. *J Lipid Res* **59**, 250-260 (2018).

13 Sextius, P. *et al.* Large scale study of epidermal recovery after stratum corneum removal: dynamics of genomic response. *Exp Dermatol* **19**, 259-268 (2010).

14 Danso, M. O., Berkers, T., Mieremet, A., Hausil, F. & Bouwstra, J. A. An ex vivo human skin model for studying skin barrier repair. *Exp. Dermatol* **24**, 48-54 (2015).

15 Berkers, T., Visscher, D., Gooris, G. S. & Bouwstra, J. A. Degree of Skin Barrier Disruption Affects Lipid Organization in Regenerated Stratum Corneum. *Acta Derm Venereol* **98**, 421-427 (2018).

16 Pinkus, H. Examination of the epidermis by the strip method of removing horny layers. I. Observations on thickness of the horny layer, and on mitotic activity after stripping. *J Invest Dermatol* **16**, 383-386 (1951).

17 Boiten, W., Absalah, S., Vreeken, R., Bouwstra, J. & van, S. J. Quantitative analysis of ceramides using a novel lipidomics approach with three dimensional response modelling. *Biochim. Biophys. Acta* **1861**, 1652-1661 (2016).

18 Boncheva, M., Damien, F. & Normand, V. Molecular organization of the lipid matrix in intact Stratum corneum using ATR-FTIR spectroscopy. *Biochim Biophys Acta* **1778**, 1344-1355 (2008).

19 Motta, S. *et al.* Ceramide composition of the psoriatic scale. *Biochim Biophys Acta* **1182**, 147-151 (1993).

20 Ishikawa, J. *et al.* Changes in the ceramide profile of atopic dermatitis patients. *J.*

*Invest Dermatol* **130**, 2511-2514 (2010).
21 Grubauer, G., Feingold, K. R., Harris, R. M. & Elias, P. M. Lipid content and lipid type as determinants of the epidermal permeability barrier. *Journal of lipid research* **30**, 89-96 (1989).
22 Uchida, Y. *et al.* Epidermal sphingomyelins are precursors for selected stratum corneum ceramides. *J Lipid Res* **41**, 2071-2082 (2000).
23 van Smeden, J. *et al.* In situ visualization of glucocerebrosidase in human skin tissue: zymography versus activity-based probe labeling. *J Lipid Res* **58**, 2299-2309 (2017).
24 Lin, T. K., Zhong, L. & Santiago, J. L. Anti-Inflammatory and Skin Barrier Repair Effects of Topical Application of Some Plant Oils. *Int J Mol Sci* **19** (2017).
25 Tanaka, M., Zhen, Y. X. & Tagami, H. Normal recovery of the stratum corneum barrier function following damage induced by tape stripping in patients with atopic dermatitis. *Br J Dermatol* **136**, 966-967 (1997).
26 Dickel, H., Gambichler, T., Kamphowe, J., Altmeyer, P. & Skrygan, M. Standardized tape stripping prior to patch testing induces upregulation of Hsp90, Hsp70, IL-33, TNF-alpha and IL-8/CXCL8 mRNA: new insights into the involvement of 'alarmins'. *Contact Dermatitis* **63**, 215-222 (2010).
27 Nickoloff, B. J. & Naidu, Y. Perturbation of epidermal barrier function correlates with initiation of cytokine cascade in human skin. *J Am Acad Dermatol* **30**, 535-546 (1994).
28 Ogawa, E., Sato, Y., Minagawa, A. & Okuyama, R. Pathogenesis of psoriasis and development of treatment. *J Dermatol* (2017).
29 Kouris, A. *et al.* Proinflammatory cytokine responses in patients with psoriasis. *Eur Cytokine Netw* **25**, 63-68 (2014).
30 Danso, M. O. *et al.* TNF-alpha and Th2 cytokines induce atopic dermatitis-like features on epidermal differentiation proteins and stratum corneum lipids in human skin equivalents. *The Journal of investigative dermatology* **134**, 1941-1950 (2014).
31 Tawada, C. *et al.* Interferon-gamma decreases ceramides with long-chain fatty acids: possible involvement in atopic dermatitis and psoriasis. *J Invest Dermatol* **134**, 712-718 (2014).
32 van Smeden, J. & Bouwstra, J. A. Stratum Corneum Lipids: Their Role for the Skin Barrier Function in Healthy Subjects and Atopic Dermatitis Patients. *Curr Probl Dermatol* **49**, 8-26 (2016).
33 van Smeden, J. *et al.* The importance of free fatty acid chain length for the skin barrier function in atopic eczema patients. *Exp. Dermatol* **23**, 45-52 (2014).
34 van Smeden, J. *et al.* Intercellular skin barrier lipid composition and organization in Netherton syndrome patients. *J Invest Dermatol* **134**, 1238-1245 (2014).
35 van Smeden, J., Janssens, M., Gooris, G. S. & Bouwstra, J. A. The important role of stratum corneum lipids for the cutaneous barrier function. *Biochim. Biophys. Acta* **1841**, 295-313 (2014).

# 3 Supplementals chapter 3

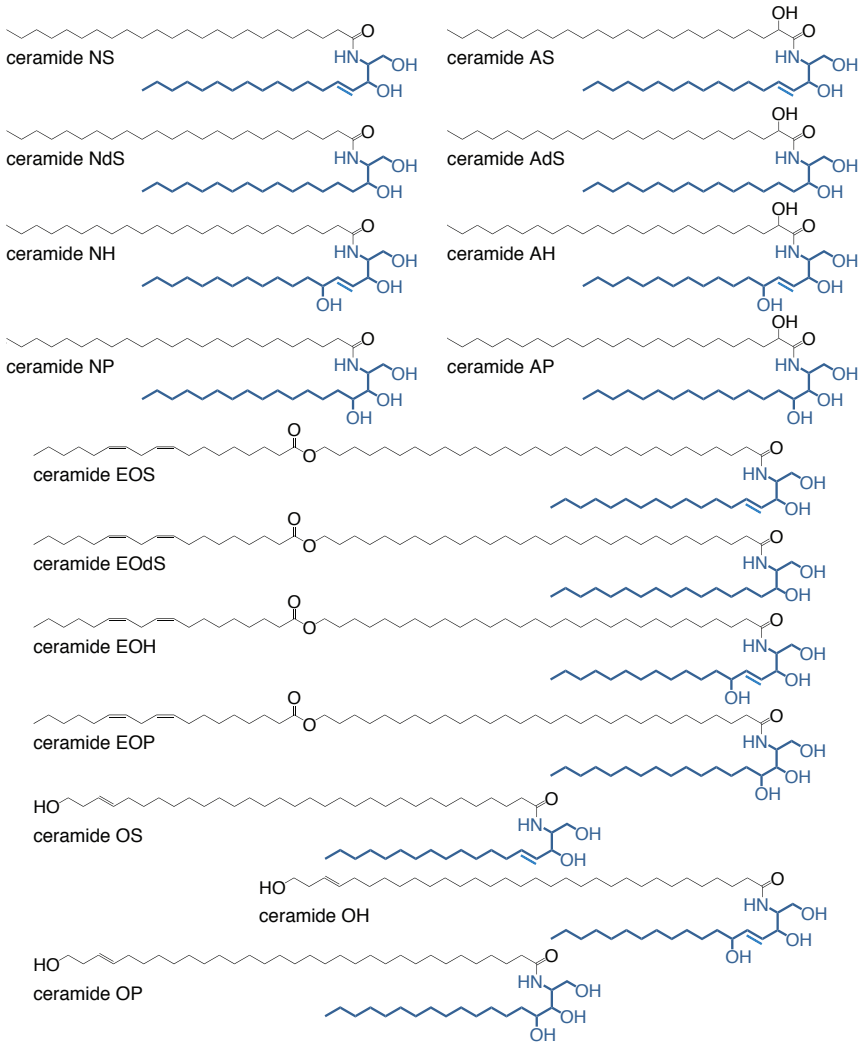


***Supplemental S3.1: Ceramides subclasses in the stratum corneum lipid matrix***

*Ceramides consist of a sphingoid base coupled to an acyl chain, which can both vary in molecular structure. ceramides are named according to their molecular structure. The sphingoid base can either be a sphingosine (S), dihydrosphingosine (dS), phytosphingosine (P), 6-hydroxysphingosine (H), whereas the acyl chain is either non-hydroxylated (N), α-hydroxylated (A), ω-hydroxylated (O), or esterified ω-hydroxylated (EO). Both the sphingoid base (blue) and the fatty acid chain (black) can vary in number of carbon atoms.*

**Supplemental S3.2: Synthetic ceramides that were used as calibrators for LC/MS analysis.**

*Numbers in brackets indicate the number of carbon atoms in the fatty acid chain and sphingosine chain, respectively.*

| Ceramides | | | |
|---|---|---|---|
| N(24)dS(18) [1] | N(20)S(18) [1] | A(24)S(18) [1] | E(18:2)O(30)S(18) [2] |
| N(18)dS(18) [1] | N(18)S(18) [1] | A(22)S(18) [1] | E(18:2)O(27)S(18) [2] |
| N(16)dS(18) [1] | N(16)S(18) [1] | A(16)S(18) [1] | E(18:2)O(30)P(S18) [2] |
| N(24)S(18) [2] | N(24)P(18) [2] | A(24)P(18) [1] | E(18:2)O(27)P(18) [2] |
| N(22)S(18) [1] | N(16)P(18) [2] | | N(24deu)S(18) [2] |

[1] Avanti polar lipids (Alabaster, USA) [2] Evonik Industries (Essen, Germany)

***Supplemental S3.3: Output of linear mixed models comparing the subclass composition.***

*$Ctrl^{in\ vivo}$ was set as the intercept of the model and the value is the mean molar percentage of selected ceramide subclass. The effect size of regeneration, ex vivo and cultured indicates the molar percentage with which the variable changes the intercept. The nested term (reg.(cu.l(exv.))) compares effect size of regeneration in vivo to the effect size of regeneration ex vivo.*

| | NdS | | NS | | NP | | NH | |
|---|---|---|---|---|---|---|---|---|
| | estimate | p-value | estimate | p-value | estimate | p-value | estimate | p-value |
| intercept ($Ctrl^{in\ vivo}$) | 10.391 | <0.001 | 9.647 | <0.001 | 22.408 | <0.001 | 16.588 | <0.001 |
| regeneration | -2.220 | <0.001 | 5.387 | <0.001 | -6.312 | <0.001 | -1.899 | 0.015 |
| *ex vivo* | -0.919 | 0.173 | -2.573 | 0.249 | 6.126 | 0.003 | -0.849 | 0.623 |
| cultured | -1.936 | <0.001 | 8.838 | <0.001 | -7.988 | <0.001 | -1.876 | 0.199 |
| reg.(cul(evx.) | 1.791 | <0.001 | 8.173 | <0.001 | -0.035 | 0.977 | -2.120 | 0.113 |

| | AdS | | AS | | AP | | AH | |
|---|---|---|---|---|---|---|---|---|
| | estimate | p-value | estimate | p-value | estimate | p-value | estimate | p-value |
| intercept ($Ctrl^{in\ vivo}$) | 1.378 | <0.001 | 4.669 | <0.001 | 11.829 | <0.001 | 13.915 | <0.001 |
| regeneration | -0.180 | 0.015 | 4.935 | <0.001 | -2.023 | 0.001 | 0.353 | 0.456 |
| *ex vivo* | -0.094 | 0.674 | -1.382 | 0.299 | 2.573 | 0.150 | -3.524 | 0.002 |
| cultured | -0.294 | 0.038 | 5.596 | <0.001 | -2.951 | 0.011 | 0.183 | 0.842 |
| reg.(cul(evx.) | 0.415 | 0.002 | -0.820 | 0.431 | -1.757 | 0.086 | -3.037 | 0.001 |

| | EOdS | | EOS | | EOP | | EOH | |
|---|---|---|---|---|---|---|---|---|
| | estimate | p-value | estimate | p-value | estimate | p-value | estimate | p-value |
| intercept ($Ctrl^{in\ vivo}$) | 0.341 | <0.001 | 4.298 | <0.001 | 0.846 | <0.001 | 2.391 | <0.001 |
| regeneration | -0.040 | 0.241 | 1.140 | <0.001 | -0.145 | 0.024 | 0.184 | 0.122 |
| *ex vivo* | 0.429 | 0.007 | -0.905 | 0.288 | 0.982 | <0.001 | 0.350 | 0.435 |
| cultured | -0.162 | 0.020 | 0.202 | 0.598 | -0.531 | <0.001 | -0.634 | 0.009 |
| reg.(cul(evx.) | -0.197 | 0.003 | -1.137 | 0.003 | -0.406 | 0.001 | -1.116 | <0.001 |

***Table S3.3 contiued***

| | OS | | OP | | OH | |
|---|---|---|---|---|---|---|
| | estimate | p-value | estimate | p-value | estimate | p-value |
| intercept (Ctrl$^{in\ vivo}$) | 0.483 | <0.001 | 0.119 | <0.001 | 0.696 | <0.001 |
| regeneration | 0.501 | <0.001 | 0.174 | <0.001 | 0.145 | 0.002 |
| *ex vivo* | -0.164 | 0.511 | 0.270 | <0.001 | -0.349 | 0.031 |
| cultured | 0.830 | 0.001 | 0.018 | 0.761 | 0.317 | 0.001 |
| reg.(cul(evx.) | 0.694 | 0.002 | -0.063 | 0.243 | -0.098 | 0.199 |

### *Supplemental S3.4: Output of linear mixed models for omega-hydroxylated ceramides and mean chain length*

*Ctrl$^{in\ vivo}$ was set as the intercept of the model and the effect sizes of the variable are given. The nested term compares effect size of regeneration in vivo to that of regeneration ex vivo.*

| | EO | | O | | EO+O | | MCL | |
|---|---|---|---|---|---|---|---|---|
| | estimate | p-value | estimate | p-value | estimate | p-value | estimate | p-value |
| intercept (Ctrl$^{in\ vivo}$) | 7.876 | <0.001 | 1.298 | <0.001 | 9.174 | <0.001 | 46.9 | <0.001 |
| regeneration | 1.139 | <0.001 | 0.820 | <0.001 | 1.959 | <0.001 | -0.4 | 0.010 |
| *ex vivo* | 0.856 | 0.545 | -0.213 | 0.559 | 0.643 | 0.685 | 0.3 | 0.522 |
| cultured | -1.140 | 0.041 | 1.202 | <0.001 | 0.063 | 0.900 | -0.4 | 0.094 |
| reg.(cul(evx.) | -2.840 | <0.001 | 0.597 | 0.012 | -2.245 | <0.001 | -0.6 | 0.017 |

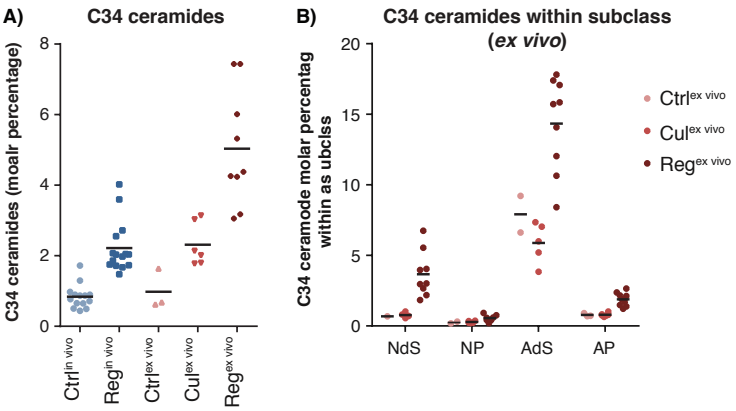


### *Supplemental S3.5: C34 ceramides percentages*

*The total amount of all ceramides was set at 100%. **A:** The level of C34 ceramides as percentage of the total ceramide content. **B:** The level of C34 ceramides as molar percentage within each subclass. These four subclasses could only reliably detect in ex vivo skin SC samples. Lines are the mean.*

| | estimate | p-value |
|---|---|---|
| intercept (Ctrl$^{in\ vivo}$) | 0.84 | 0.001 |
| regeneration | 1.38 | <0.001 |
| *ex vivo* | 0.14 | 0.804 |
| cultured | 1.41 | 0.025 |
| reg.(cul(evx.) | 1.26 | 0.028 |

### *Supplemental 3.6: Output of the liner mixed model comparing total C34 ceramide molar percentage*

*Ctrl$^{in\ vivo}$ was set as the intercept of the model and the effect sizes of the other variable are given. The nested term compares effect size of regeneration in vivo to the effect size of regeneration ex vivo.*

### *SupplementalS3.7: Output of the linear mixed models for C34 ceramides within its subclass*

*The first part of the table specifies the F-test type III effects. Indicating if parameters were significantly changed independent of interaction variables. Here showing that regeneration is significantly affects C34 % within the subclasses, independent of sample type or which subclass is selected. Second part of the table shows the specific estimates of fixed effects with Ctrl$^{in\ vivo}$ set as intercept. The effect sizes of regeneration, ex vivo, and cultured are indicated with significance. The nested interaction variable indicates if the changes due to regeneration were different for ex vivo samples.*

**C34 ceramide percentage per subclass F-test of type III effects**

| Source | F | Sig. | | F | Sig. |
|---|---|---|---|---|---|
| intercept | 298.650 | <0.001 | *ex vivo* * subclass | 0.401 | 0.753 |
| regenerated | 31.825 | <0.001 | cultured * subclass | 1.083 | 0.360 |
| cultured | 4.477 | 0.037 | reg* subclass | 2.425 | 0.070 |
| *ex vivo* | 0.114 | 0.737 | reg.(cul(evx.) | 1.508 | 0.222 |
| subclass | 92.262 | <0.001 | reg.*subclass(cul(evx.) | 0.899 | 0.445 |

| Parameter estimate | **NS C34%** | | **AS C34%** | | **NH C34%** | | **AH C34%** | |
|---|---|---|---|---|---|---|---|---|
| | estimate | p-value | estimate | p-value | estimate | p-value | estimate | p-value |
| intercept (Ctrl$^{in\ vivo}$) | 1.60 | 0.033 | 10.58 | <0.001 | 1.40 | 0.050 | 1.30 | 0.055 |
| regeneration | 1.15 | 0.153 | 1.76 | 0.008 | 0.91 | 0.243 | 1.42 | 0.056 |
| *ex vivo* | 1.40 | 0.340 | -0.06 | 0.963 | -0.71 | 0.623 | -0.32 | 0.843 |
| cultured | 3.06 | 0.015 | 0.51 | 0.682 | 0.20 | 0.873 | 0.65 | 0.647 |
| reg.(cul(evx.) | -0.20 | 0.868 | 2.03 | 0.075 | -0.19 | 0.877 | 1.28 | 0.283 |

| | | | 95% confidence | |
|---|---|---|---|---|
| | Size | p-value | Lower | Upper |
| Intercept | 45.32 | <0.001 | 44.89 | 45.74 |
| EOpr | 0.21 | <0.001 | 0.17 | 0.26 |
| C34pr | -0.20 | <0.001 | -0.26 | -0.15 |

### *Supplemental S3.8: General linear model output predicting mean chain length*

*A model predicting the MCL was created using EO and C34 ceramide percentage as covariant, EOpr and C34pr, respectively. The following parameters were observed with significance and 95% confidence interval indicated.*

| | **MuCer molar%** | |
|---|---|---|
| | estimate | p-value |
| intercept (Ctrl$^{ex\ vivo}$) | 2.35 | 0.003 |
| regeneration | 3.06 | <0.001 |
| cultured | 1.45 | 0.030 |

### *Supplemental S3.9: Output of the linear mixed models for MuCer in ex vivo SC*

*Ctrl$^{ex\ vivo}$ was set as the intercept and the effect of regeneration was nested within cultured. Effect sizes are given.*

| | Stretching peak position | |
|---|---|---|
| | estimate | p-value |
| intercept (Ctrl$^{in\ vivo}$) | 2848.73 | <0.001 |
| regeneration | 0.03 | 0.799 |
| *ex vivo* | 0.50 | 0.036 |
| cultured | 0.07 | 0.836 |
| reg.(cul(evx.) | 0.30 | 0.423 |

***Supplemental S3.10: Outcome of the linear mixed models for lipid ordering in the SC matrix***

*The intercept indicates the mean of the peak position for the stretching vibrations in the Ctrl$^{in\ vivo}$ sample. The effect size indicates the change of the peak position relative to the intercept.*

| | | | 95% confidence | |
|---|---|---|---|---|
| | Size | p-value | Lower | Upper |
| Intercept | 2847.93 | 0.000 | 2846.94 | 2848.92 |
| C34pr | 0.30 | 0.001 | 0.14 | 0.46 |
| EOpr | -0.02 | 0.602 | -0.08 | 0.05 |
| Subratio | 0.13 | 0.017 | 0.02 | 0.24 |

***Supplemental S3.11: General linear model output predicting $CH_2$ stretching peak position of the FTIR spectrum.***

*A model to predict the $CH_2$ stretching peak position was made using the molar ratio dS+P+H/S between the sphingoid base of the ceramide (excluding EO ceramides), EO ceramide percentage, and C34 ceramide percentage as covariates. The following parameters were observed with significance and 95% confidence interval indicated.*

***Supplemental S3.12***

*Chemicals*

For culturing the SkinBaR models the following chemicals and materials were used: Cyanoacrylate (Bison, Goes, the Netherlands), DMEM, Ham's F12, and penicillin/streptomycin were obtained from Fisher Scientific (Waltham, Massachusetts, USA), bovine serum albumin, sodium bromide, ethanol, acetone, trypsin, trypsin inhibitor, selenious acid, hydrocortisone, isoproterenol, L-carnitine, L-serine, insulin, α-tocopherol acetate, ascorbic acid, arachidonic acid, linoleic acid, and palmitic acid were purchased from Sigma-Aldrich (Zwijndrecht, the Netherlands).

For SC lipid extraction and LC/MS analysis the following solvents were purchased: methanol and chloroform were obtained from Lab-Scan (HPLC grade, Gliwice, Poland), isopropanol and ethanol were bought from Biosolve (UPLC grade, Valkenswaard, the Netherlands), and heptane was acquired from Actu-All (HPLC grade, Oss, the Netherlands). The synthetic ceramide listed in supplemental S3.2 were used as calibrators for LC/MS analysis.

*Inclusion and exclusion criteria for in vivo study*

Prior inclusion, a dermatologist checked whether the volunteer was eligible for participation. Exclusion criteria were: (history of) dermatological disorders, chronic inflammatory disease, use of systemic drug therapies, abundant hair or unnatural abnormalities on the ventral forearm, (history of) drug abuse, and pregnancy.

*Stratum corneum isolation from ex vivo skin*

SC was isolated from the *ex vivo* skin samples by placing the skin overnight in a 0.1% trypsin solution in PBS (pH 7.4) and 1 hour at 37°C. Subsequently, the SC was peeled off, washed in 0.1% trypsin inhibitor solution, and twice in Millipore water.

*FTIR analysis*

All measurements were performed on a spectrometer equipped with a broadband mercury-cadmium-telluride detector cooled with liquid $N_2$. Dry air constantly purged the sample compartments. Due to practical reasons, spectra for the *in vivo* SC and the SkinBaR SC were collected in reflection and transmission mode, respectively.

*In vivo samples:*

In order to measure the lipid organization in the SC on the arms of the volunteers, attenuated total reflection FTIR (ATR-FTIR) was used. The spectrometer was connected to an external ATR accessory with a single reflection diamond (GladiATR, PIKE technologies, Maddison USA). Each spectrum was an average of 150 scans with a spectral resolution of 2 $cm^{-1}$ measured at skin temperature. The instrument software Resolutions Pro 4.1 (Agilent Technologies) was used for data treatment. The center of gravity of the $CH_2$ symmetric stretching peak was determined at 90% of the peak height to determine the lateral ordering of the lipids. The centers of gravity 5 spectra were combined (e.g. after tape 2-10, and after tape 12-20) for analysis.

*Ex vivo samples:*

24 hours prior to data collection, the isolated SC sheets were hydrated over a 27% NaBr solution in $D_2O$ at room temperature. After hydration, the SC sheet was sandwiched between two AgBr-windows and measured in transmission mode. During the measurement, the sample temperature increased from 0 to 90°C. Spectra were recorded during 2 minutes at a 1°C interval, and as a co-addition of 128 scans using 1 $cm^{-1}$ resolution. The center of gravity of the $CH_2$ symmetric stretching peak at skin temperature (32°C) was determined as described above.

*Statistical analysis*

*Linear mixed models*

LMM were used in order to compare the means of several variables regarding CER composition and lipid organization between the five sample groups. The models were setup so that the effect of regeneration *in vivo* could be compared to regeneration *ex vivo*. Three variables were chosen as fixed factors: I) if the sample was *in vivo* or *ex vivo (*Ex vivo*)*, II) if the SC was regenerated or not, and III) if the sample was cultured or not. To accommodate and test for the possibility that regeneration had a different effect *in vivo* compared to *ex vivo*, a separate nested factor for regeneration was created. Nesting was performed to obtain reliable F-test statistics. This regeneration factor was nested in culturing which was nested in *ex vivo*. This because only *ex vivo* skin can be cultured and for ex vivo skin only cultured *ex vivo* skin can be regenerated. The resulting term compares the effect size of regeneration *in vivo* (difference between $Ctrl^{in\ vivo}$ and $Reg^{in\ vivo}$) to the effect of regeneration in the SkinBar model (difference between $Cul^{ex\ vivo}$ and $Reg^{ex\ vivo}$). The starting point of the models (intercept) was chosen to be the *in vivo* control samples.

*w*

*General linear models*

General linear modeling was performed to compare a variable (like MCL) with multiple other variables. These are set as covariates, without interactions, and with prediction of the intercept.

These models predict the amount of change (in MCL) caused by the other parameters (for MCL molar fraction of EO and C34 ceramide) which is added to the intercept To obtain a predictive model for the $CH_2$ stretching peak position we chose variables that have previously been used or are expected to affect the lipid ordering. C34 and EO percentage were chosen, as both have been related to lipid organization[1] and they are predictors of the average chain length [1] therefore omitting the mean chain length in the model. Ratios between the subclasses have been shown to affect the lipid organization[2-4]. Here, the  ratio was chosen which is an expression of sphingoid bases, as EO ceramides are included as a separate factor these were left out of this ratio. The model uses these 3 parameters as covariant.



**Supplemental references:**


1 Janssens, M. *et al.* Increase in short-chain ceramides correlates with an altered lipid organization and decreased barrier function in atopic eczema patients. *J. Lipid Res* **53**, 2755-2766 (2012).

2 Boiten, W. A. *et al.* Applying a vernix caseosa based formulation accelerates skin barrier repair by modulating lipid biosynthesis. *J Lipid Res* **59**, 250-260 (2018).

3 Groen, D., Poole, D. S., Gooris, G. S. & Bouwstra, J. A. Investigating the barrier function of skin lipid models with varying compositions. *European journal of pharmaceutics and biopharmaceutics : official journal of Arbeitsgemeinschaft fur Pharmazeutische Verfahrenstechnik e.V* **79**, 334-342 (2011).

4 Skolova, B., Kovacik, A., Tesar, O., Opalka, L. & Vavrova, K. Phytosphingosine, sphingosine and dihydrosphingosine ceramides in model skin lipid membranes: permeability and biophysics. *Biochimica et biophysica acta* **1859**, 824-834 (2017).